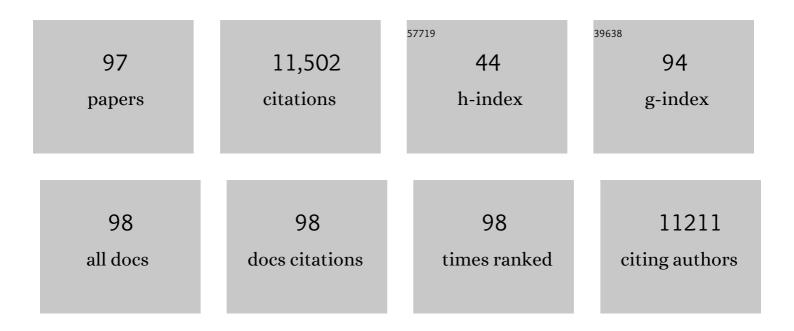
## Liming Zhou

List of Publications by Year in descending order

Source: https://exaly.com/author-pdf/5750204/publications.pdf Version: 2024-02-01



#	Article	IF	CITATIONS
1	Variations in northern vegetation activity inferred from satellite data of vegetation index during 1981 to 1999. Journal of Geophysical Research, 2001, 106, 20069-20083.	3.3	1,244
2	Surface Urban Heat Island Across 419 Global Big Cities. Environmental Science & Technology, 2012, 46, 696-703.	4.6	864
3	Evidence for a significant urbanization effect on climate in China. Proceedings of the National Academy of Sciences of the United States of America, 2004, 101, 9540-9544.	3.3	709
4	Variations in satellite-derived phenology in China's temperate vegetation. Global Change Biology, 2006, 12, 672-685.	4.2	643
5	A large carbon sink in the woody biomass of Northern forests. Proceedings of the National Academy of Sciences of the United States of America, 2001, 98, 14784-14789.	3.3	568
6	Remote sensing of vegetation and land-cover change in Arctic Tundra Ecosystems. Remote Sensing of Environment, 2004, 89, 281-308.	4.6	522
7	Afforestation in China cools local land surface temperature. Proceedings of the National Academy of Sciences of the United States of America, 2014, 111, 2915-2919.	3.3	501
8	Evaporative cooling over the Tibetan Plateau induced by vegetation growth. Proceedings of the National Academy of Sciences of the United States of America, 2015, 112, 9299-9304.	3.3	404
9	Interannual variations of monthly and seasonal normalized difference vegetation index (NDVI) in China from 1982 to 1999. Journal of Geophysical Research, 2003, 108, .	3.3	401
10	Widespread decline of Congo rainforest greenness in the past decade. Nature, 2014, 509, 86-90.	13.7	351
11	Climate mitigation from vegetation biophysical feedbacks during the past three decades. Nature Climate Change, 2017, 7, 432-436.	8.1	323
12	Climate Response to Rapid Urban Growth: Evidence of a Human-Induced Precipitation Deficit. Journal of Climate, 2007, 20, 2299-2306.	1.2	300
13	Divergent hydrological response to large-scale afforestation and vegetation greening in China. Science Advances, 2018, 4, eaar4182.	4.7	287
14	Changes in vegetation net primary productivity from 1982 to 1999 in China. Global Biogeochemical Cycles, 2005, 19, n/a-n/a.	1.9	244
15	Impacts of wind farms on land surface temperature. Nature Climate Change, 2012, 2, 539-543.	8.1	228
16	Effect of climate and CO2changes on the greening of the Northern Hemisphere over the past two decades. Geophysical Research Letters, 2006, 33, .	1.5	207
17	Increasing net primary production in China from 1982 to 1999. Frontiers in Ecology and the Environment, 2003, 1, 293-297.	1.9	195
18	Precipitation patterns alter growth of temperate vegetation. Geophysical Research Letters, 2005, 32, .	1.5	179

#	Article	IF	CITATIONS
19	Multiscale analysis and validation of the MODIS LAI productl. Uncertainty assessment. Remote Sensing of Environment, 2002, 83, 414-430.	4.6	174
20	Effect of orbital drift and sensor changes on the time series of AVHRR vegetation index data. IEEE Transactions on Geoscience and Remote Sensing, 2000, 38, 2584-2597.	2.7	151
21	Impact of vegetation removal and soil aridation on diurnal temperature range in a semiarid region: Application to the Sahel. Proceedings of the National Academy of Sciences of the United States of America, 2007, 104, 17937-17942.	3.3	151
22	Spatial dependence of diurnal temperature range trends on precipitation from 1950 to 2004. Climate Dynamics, 2009, 32, 429-440.	1.7	139
23	Changes in biomass carbon stocks in China's grasslands between 1982 and 1999. Clobal Biogeochemical Cycles, 2007, 21, n/a-n/a.	1.9	127
24	Change in snow phenology and its potential feedback to temperature in the Northern Hemisphere over the last three decades. Environmental Research Letters, 2013, 8, 014008.	2.2	125
25	Analysis of interannual changes in northern vegetation activity observed in AVHRR data from 1981 to 1994. IEEE Transactions on Geoscience and Remote Sensing, 2002, 40, 115-130.	2.7	122
26	Observational evidence of sensitivity of surface climate changes to land types and urbanization. Geophysical Research Letters, 2005, 32, n/a-n/a.	1.5	112
27	China experiencing the recent warming hiatus. Geophysical Research Letters, 2015, 42, 889-898.	1.5	111
28	Possible causes of the Central Equatorial African long-term drought. Environmental Research Letters, 2016, 11, 124002.	2.2	100
29	Sunlight mediated seasonality in canopy structure and photosynthetic activity of Amazonian rainforests. Environmental Research Letters, 2015, 10, 064014.	2.2	90
30	Multiscale analysis and validation of the MODIS LAI productII. Sampling strategy. Remote Sensing of Environment, 2002, 83, 431-441.	4.6	89
31	Satellite-indicated long-term vegetation changes and their drivers on the Mongolian Plateau. Landscape Ecology, 2015, 30, 1599-1611.	1.9	88
32	Analysis of a multiyear global vegetation leaf area index data set. Journal of Geophysical Research, 2002, 107, ACL 14-1.	3.3	85
33	Detection and attribution of anthropogenic forcing to diurnal temperature range changes from 1950 to 1999: comparing multi-model simulations with observations. Climate Dynamics, 2010, 35, 1289-1307.	1.7	84
34	Observational Quantification of Climatic and Human Influences on Vegetation Greening in China. Remote Sensing, 2017, 9, 425.	1.8	81
35	Widespread increase of boreal summer dry season length over the Congo rainforest. Nature Climate Change, 2019, 9, 617-622.	8.1	70
36	Assessing reanalysis data for understanding rainfall climatology and variability over Central Equatorial Africa. Climate Dynamics, 2019, 53, 651-669.	1.7	61

#	Article	IF	CITATIONS
37	Stronger warming amplification over drier ecoregions observed since 1979. Environmental Research Letters, 2015, 10, 064012.	2.2	60
38	Evaluation of simulated climatological diurnal temperature range in CMIP5 models from the perspective of planetary boundary layer turbulent mixing. Climate Dynamics, 2017, 49, 1-22.	1.7	52
39	A 3D Canopy Radiative Transfer Model for Global Climate Modeling: Description, Validation, and Application. Journal of Climate, 2014, 27, 1168-1192.	1.2	49
40	Validation of Satellite Precipitation Estimates over the Congo Basin. Journal of Hydrometeorology, 2019, 20, 631-656.	0.7	49
41	Evaporative water loss of 1.42 million global lakes. Nature Communications, 2022, 13, .	5.8	49
42	Impact of Vegetation Types on Surface Temperature Change. Journal of Applied Meteorology and Climatology, 2008, 47, 411-424.	0.6	48
43	Diurnal and seasonal variations of wind farm impacts on land surface temperature over western Texas. Climate Dynamics, 2013, 41, 307-326.	1.7	48
44	Satellite Observations of Wind Farm Impacts on Nocturnal Land Surface Temperature in Iowa. Remote Sensing, 2014, 6, 12234-12246.	1.8	46
45	A case study of effects of atmospheric boundary layer turbulence, wind speed, and stability on wind farm induced temperature changes using observations from a field campaign. Climate Dynamics, 2016, 46, 2179-2196.	1.7	46
46	Spatiotemporal patterns of changes in maximum and minimum temperatures in multiâ€model simulations. Geophysical Research Letters, 2009, 36, .	1.5	45
47	Understanding the Central Equatorial African long-term drought using AMIP-type simulations. Climate Dynamics, 2018, 50, 1115-1128.	1.7	44
48	Mechanisms for stronger warming over drier ecoregions observed since 1979. Climate Dynamics, 2016, 47, 2955-2974.	1.7	40
49	Desert Amplification in a Warming Climate. Scientific Reports, 2016, 6, 31065.	1.6	36
50	Assessing climatic impacts of future land use and land cover change projected with the CanESM2 model. International Journal of Climatology, 2015, 35, 3661-3675.	1.5	34
51	Increasing extent and intensity of thunderstorms observed over the Congo Basin from 1982 to 2016. Atmospheric Research, 2018, 213, 17-26.	1.8	34
52	Sensitivity of simulated terrestrial carbon assimilation and canopy transpiration to different stomatal conductance and carbon assimilation schemes. Climate Dynamics, 2011, 36, 1037-1054.	1.7	33
53	Changes in cloudiness over the Amazon rainforests during the last two decades: diagnostic and potential causes. Climate Dynamics, 2011, 37, 1151-1164.	1.7	32
54	An Externally Forced Decadal Rainfall Seesaw Pattern Over the Sahel and Southeast Amazon. Geophysical Research Letters, 2019, 46, 923-932.	1.5	31

#	Article	IF	CITATIONS
55	Regional air pollution brightening reverses the greenhouse gases induced warmingâ€elevation relationship. Geophysical Research Letters, 2015, 42, 4563-4572.	1.5	30
56	Detection of urbanization signals in extreme winter minimum temperature changes over Northern China. Climatic Change, 2014, 122, 595-608.	1.7	29
57	Observed Thermal Impacts of Wind Farms Over Northern Illinois. Sensors, 2015, 15, 14981-15005.	2.1	29
58	New Rainfall Datasets for the Congo Basin and Surrounding Regions. Journal of Hydrometeorology, 2018, 19, 1379-1396.	0.7	28
59	Simulating Impacts of Real-World Wind Farms on Land Surface Temperature Using the WRF Model: Validation with Observations. Monthly Weather Review, 2017, 145, 4813-4836.	0.5	26
60	Simulating impacts of real-world wind farms on land surface temperature using the WRF model: physical mechanisms. Climate Dynamics, 2019, 53, 1723-1739.	1.7	26
61	Spatiotemporal Structure of Wind Farm-atmospheric Boundary Layer Interactions. Energy Procedia, 2013, 40, 530-536.	1.8	25
62	Satellite Observations of El Niño Impacts on Eurasian Spring Vegetation Greenness during the Period 1982–2015. Remote Sensing, 2017, 9, 628.	1.8	24
63	Impacts of increased urbanization on surface temperature, vegetation, and aerosols over Bengaluru, India. Remote Sensing Applications: Society and Environment, 2019, 16, 100261.	0.8	23
64	Detecting Wind Farm Impacts on Local Vegetation Growth in Texas and Illinois Using MODIS Vegetation Greenness Measurements. Remote Sensing, 2017, 9, 698.	1.8	20
65	Changing response of the North Atlantic/European winter climate to the 11 year solar cycle. Environmental Research Letters, 2018, 13, 034007.	2.2	20
66	A threeâ€dimensional analytic model for the scattering of a spherical bush. Journal of Geophysical Research, 2008, 113, .	3.3	19
67	Effects of Topography on Assessing Wind Farm Impacts Using MODIS Data. Earth Interactions, 2013, 17, 1-18.	0.7	19
68	Impact of precipitationâ€induced sensible heat on the simulation of landâ€surface air temperature. Journal of Advances in Modeling Earth Systems, 2014, 6, 1311-1320.	1.3	19
69	Trends in Tropical Wave Activity from the 1980s to 2016. Journal of Climate, 2019, 32, 1661-1676.	1.2	19
70	Asymmetric response of maximum and minimum temperatures to soil emissivity change over the Northern African Sahel in a GCM. Geophysical Research Letters, 2008, 35, .	1.5	18
71	Observed changes in fire patterns and possible drivers over Central Africa. Environmental Research Letters, 2020, 15, 0940b8.	2.2	18
72	Observational Evidence for Desert Amplification Using Multiple Satellite Datasets. Scientific Reports, 2017, 7, 2043.	1.6	17

#	Article	IF	CITATIONS
73	Hotspots of the sensitivity of the land surface hydrological cycle to climate change. Science Bulletin, 2013, 58, 3682-3688.	1.7	16
74	Response to Comment on "Surface Urban Heat Island Across 419 Global Big Cities― Environmental Science & Technology, 2012, 46, 6889-6890.	4.6	15
75	Dynamics of leaf area for climate and weather models. Journal of Geophysical Research, 2008, 113, .	3.3	14
76	Empirical Evidence for Impacts of Internal Migration on Vegetation Dynamics in China from 1982 to 2000. Sensors, 2008, 8, 5069-5080.	2.1	13
77	The MJO's impact on rainfall trends over the Congo rainforest. Climate Dynamics, 2020, 54, 2683-2695.	1.7	12
78	Rising Planetary Boundary Layer Height over the Sahara Desert and Arabian Peninsula in a Warming Climate. Journal of Climate, 2021, 34, 4043-4068.	1.2	12
79	Increasing Influence of Indian Ocean Dipole on Precipitation Over Central Equatorial Africa. Geophysical Research Letters, 2021, 48, e2020GL092370.	1.5	11
80	Vegetation Greening Offsets Urbanizationâ€Induced Fast Warming in Guangdong, Hong Kong, and Macao Region (GHMR). Geophysical Research Letters, 2021, 48, e2021GL095217.	1.5	11
81	Diurnal asymmetry of desert amplification and its possible connections to planetary boundary layer height: a case study for the Arabian Peninsula. Climate Dynamics, 2021, 56, 3131-3156.	1.7	11
82	Reconciling Human and Natural Drivers of the Tripole Pattern of Multidecadal Summer Temperature Variations Over Eurasia. Geophysical Research Letters, 2021, 48, e2021GL093971.	1.5	10
83	Land–atmosphere–aerosol coupling in North China during 2000–2013. International Journal of Climatology, 2017, 37, 1297-1306.	1.5	8
84	Analyzing intensifying thunderstorms over the Congo Basin using the Gálvez-Davison index from 1983–2018. Climate Dynamics, 2021, 56, 949-967.	1.7	8
85	Effects of Nonuniform Land Surface Warming on Summer Anomalous Extratropical Cyclone Activity and the East Asian Summer Monsoon: Numerical Experiments with a Regional Climate Model. Journal of Climate, 2020, 33, 10469-10488.	1.2	8
86	Derivation of a soil albedo dataset from MODIS using principal component analysis: Northern Africa and the Arabian Peninsula. Geophysical Research Letters, 2005, 32, .	1.5	6
87	Four-stream isosector approximation for canopy radiative transfer. Journal of Geophysical Research, 2007, 112, .	3.3	6
88	High-Resolution WRF Simulation of Extreme Heat Events in Eastern China: Large Sensitivity to Land Surface Schemes. Frontiers in Earth Science, 2021, 9, .	0.8	6
89	The most extreme heat waves in Amazonia happened under extreme dryness. Climate Dynamics, 2022, 59, 281-295.	1.7	6
90	A shift in the diurnal timing and intensity of deep convection over the Congo Basin during the past 40Âyears. Atmospheric Research, 2021, 264, 105869.	1.8	4

#	Article	IF	CITATIONS
91	Orographic enhancement of rainfall over the Congo Basin. Atmospheric Science Letters, 2022, 23, .	0.8	2
92	Moisture transport and water vapour budget over the Sahara Desert. International Journal of Climatology, 2022, 42, 6829-6843.	1.5	2
93	Relationships between intense convection, lightning, and rainfall over the interior Congo Basin using TRMM data. Atmospheric Research, 2022, 273, 106164.	1.8	2
94	Spatial-temporal trend of seasonally-integrated normalized difference vegetation index as an indicator of changes in Arctic tundra vegetation in the early 1990s. , 0, , .		1
95	Recent rainfall conditions in the Congo Basin. Environmental Research Letters, 2022, 17, 054052.	2.2	1
96	Analyzing Meteorological and Chemical Conditions for Two High Ozone Events Over the New York City and Long Island Region. , 2020, , .		0
97	Weather, Climatic and Ecological Impacts of Onshore Wind Farms. , 2022, , 165-188.		0